A moss species for magnetic biomonitoring the airborne particle pollution

Una especie de musgo para el biomonitoreo magnético de la contaminación por partículas suspendidas

Débora C. **Marié**[1,2,*], Lucila **Martino**[1,2], Marcos A.E. **Chaparro**[1,2], Cristian **D'Angelo**[1,2], Juan M. **Lavornia**[3], Harald N. **Böhnel**[4]

[1] Centro de Investigaciones en Física e Ingeniería del Centro de la Provincia de Buenos Aires (CIFICEN), UNCPBA-CICPBA-CONICET, Pinto 399, 7000 Tandil, Argentina.

[2] Universidad Nacional del Centro de la Provincia de Buenos Aires (UNCPBA), Facultad de Ciencias Exactas, IFAS, Pinto 399, 7000 Tandil, Buenos Aires, Argentina.

[3] Instituto de Ciencias Polares, Ambiente y Recursos Naturales (ICPA), Universidad Nacional de Tierra del Fuego (UNTDF), Ushuaia, Argentina.

[4] Instituto de Geociencias (IGc), Universidad Nacional Autónoma de México (UNAM), Boulevard Juriquilla No. 3001, 76230 Querétaro, México.

* Corresponding author: (D.C. Marié)
deboracmarie@gmail.com

How to cite this article:
Marié, D.C., Martino, L., Chaparro, M.A.E., D'Angelo, C., Lavornia, J.M., Böhnel H.N. 2024, A moss species for magnetic biomonitoring the airborne particle pollution: Boletín de la Sociedad Geológica Mexicana, 76 (3), A040324. http://dx.doi.org/10.18268/BSGM2024v76n3a040324

Manuscript received: Septermber 29,2023
Corrected manuscript received: November 27, 2023
Manuscript accepted: December 6, 2023

Peer Reviewing under the responsibility of Universidad Nacional Autónoma de México.

ABSTRACT

The magnetic properties of eighty-four moss samples of *Orthotrichum diaphanum* Brid. collected in a medium-sized city were studied. Mosses can be considered passive collectors of air particle pollution produced by vehicular and industrial emissions because they absorb their nutrients (and pollutants) from the air. Using the environmental magnetism techniques and this moss species, we determined the most impacted areas around factories and with high vehicular traffic, where mass-specific magnetic susceptibility χ reached values of 668×10^{-8} m^3kg^{-1}. These areas presented coarser magnetic particles (0.2 – 5 μm) than avenues and street sites. The studies of magnetic mineralogy indicated that magnetite is the main magnetic carrier. Scanning electron microscopy analysis showed the presence of Fe-rich spherules and particles of different sizes and morphologies. Laser-induced breakdown spectroscopy studies determined the presence of Fe, Mn, Al, Cu, Si, and Ti, some of which correlated significantly with magnetic parameters. The statistical comparison of magnetic parameters between moss *O. diaphanum* and lichen *Parmotrema pilosum* revealed that both species are effective biological indicators for air particle monitoring.

Keywords: mosses, magnetic biomonitoring, air particle pollution, LIBS, lichens.

RESUMEN

Se estudiaron las propiedades magnéticas de ochenta y cuatro muestras de musgo Orthotrichum diaphanum Brid. colectadas en una ciudad de tamaño medio. Los musgos pueden considerarse colectores pasivos de la contaminación por partículas en el aire producida por las emisiones vehiculares e industriales porque absorben sus nutrientes (y contaminantes) del aire. Utilizando las técnicas de magnetismo ambiental y esta especie de musgo, determinamos áreas con mayor impacto alrededor de fábricas metalúrgicas y con alto tránsito vehicular, donde la susceptibilidad magnética específica χ alcanza valores de 668×10^{-8} m^3kg^{-1}. Estas áreas presentan partículas magnéticas más gruesas (0.2 – 5 μm) que en avenidas y calles. Los estudios de mineralogía magnética indican que la magnetita es el principal portador magnético. El análisis por microscopía electrónica de barrido mostró la presencia de esférulas y partículas ricas en Fe de diferentes tamaños y morfologías. Los estudios de espectroscopía de ruptura inducida por láser determinaron la presencia de Fe, Mn, Al, Cu, Si y Ti, algunos de los cuales se correlacionan significativamente con parámetros magnéticos. La comparación estadística de parámetros magnéticos entre el musgo O. diaphanum y el liquen Parmotrema pilosum reveló que ambas especies son indicadores biológicos eficaces para el monitoreo de partículas en el aire.

Palabras clave: musgos, biomonitoreo magnético, contaminación por partículas en el aire, LIBS, líquenes.

http://dx.doi.org/10.18268/BSGM2024v76n3a040324

1. Introduction

Mosses are found in most terrestrial or freshwater aquatic ecosystems. They grow in humid and shady places (forests, bark, rocks, and tree roots, among others), deserts, and polar climates because they may survive in adverse conditions. A unique characteristic is living dehydrated for years and recovering vital functions when moistened (Mahapatra *et al.*, 2019). The lack of a developed root system means that metal nutrient absorption is directly affected by atmospheric deposition (Zhou *et al.* 2017). The use of mosses for monitoring potentially toxic elements (PTE) in different areas has been used in Europe for more than 30 years due to its advantages compared with other more evolved plants (Fabian *et al.*, 2011). Among others, Calasans and Malm (1997) have conducted studies using mosses as active and passive bioindicators to estimate the deposition of atmospheric pollutants around industrial facilities.

The elemental composition of PTE trapped by mosses has usually been analyzed by atomic absorption spectroscopy and inductively coupled plasma atomic emission spectroscopy. Laser-Induced Breakdown Spectroscopy (LIBS) is an emerging low-cost and effective technique (Singh and Thakur, 2007). LIBS can perform rapid, in-situ and multi-element measurements simultaneously, requiring very little or no prior preparation of the samples to be analyzed. Recently, precise elemental determination of vegetables (*i.e.*, chard and macrophytes) was reported by Martino *et al.* (2021) and Martino and D'Angelo (2022).

Various biomonitors, such as tree leaves and epiphytic species, can accumulate airborne magnetic particles (AMP) that are measured by magnetic techniques. Hence, this methodology has been called magnetic biomonitoring (Chaparro, 2021). Magnetic biomonitoring using lichens and mosses began in the 2010s in Europe (Jordanova *et al.*, 2010; Fabián *et al.*, 2011; Salo *et al.*, 2012) and South America (Chaparro *et al.*, 2013). The mentioned authors and others have shown that magnetic biomonitoring using mosses and lichens are suitable biological sensors for assessing the spatiotemporal distribution of AMP derived from anthropogenic activities.

This work has the following main objectives: 1) to determine the magnetic properties and trace elements of moss samples collected in an urban area using environmental magnetism and LIBS techniques, 2) to detect the most impacted sites through concentration-dependent magnetic parameters, 3) to compare magnetic parameters data between this moss species and lichen samples, and analyze the use of the moss species as a valuable tool for magnetic biomonitoring.

2. Study area

The selected study area is in Tandil (37° 19.5' S, 59°08.3' W), southeast of the Buenos Aires Province (Figure 1). Tandil is a medium-sized city of 150,162 inhabitants (Instituto Nacional de Estadística y Censos, 2023), which has a per capita of approximately 0.5 vehicles (cars, trucks, and heavy transports; Sosa, 2015).

The study area is characterized by a humid subtropical climate with well-marked seasons, hot and rainy summers, and cold and dry winters. Picone and Campo, 2012; Picone, 2014; Sosa, 2015) conducted a meteorological analysis between 2001 and 2010, indicating that the annual average temperature and rainfall were 13.4 °C and 845.2 mm, respectively. The city also has an industrial area of 6 km from downtown, although some metallurgical industries are located inside the urban area (0.2 per km^2). The industrial and vehicular-derived emissions dispersed and deposited in this area have been identified as the primary sources of air particle pollutants (Chaparro *et al.*, 2002; Marié *et al.*, 2016).

A total of 84 samples of native moss were collected following a stratified sampling design. Individuals were removed using wooden tools to avoid magnetic contamination and placed in paper bags. Sampling sites, main avenues, and metallurgical industries are detailed in Figure 1. The samples

http://dx.doi.org/10.18268/BSGM2024v76n3a040324

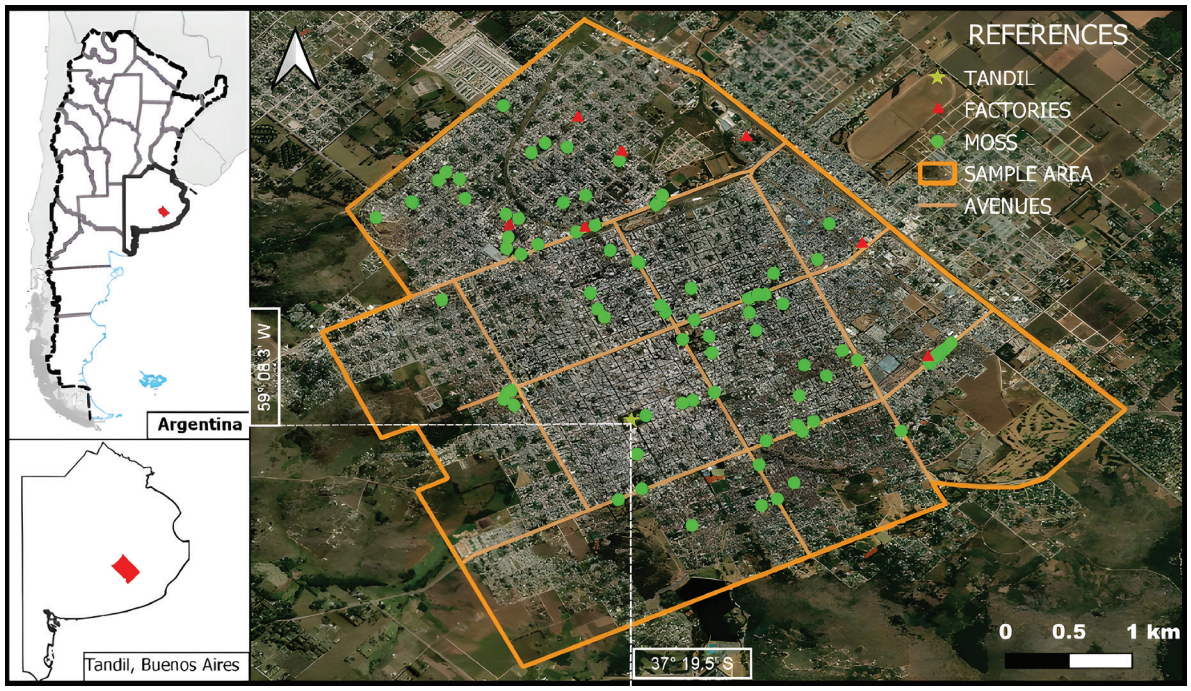

Figure 1 Tandil City, Buenos Aires Province, Argentina (59°08.3' W, 37°19.5' S), moss samples (circle), industries (triangles), and main avenues (orange lines) are shown.

were stored in the laboratory and kept dry for a week. Then, they were dried on a stove at 40°C for one day and placed in plastic containers of 8 cm^3.

3. Methodology

3.1. MOSS IDENTIFICATION

The collected individuals were hydrated, and histological sections were made to observe their external morphology under a stereoscopic microscope and histological sections of internal structures under a regular microscope. Specialized dichotomous keys were used to determine family, genus, and species (Gradstein *et al.*, 2001).

For family determination, characteristics of the basal portion, the presence of ribs, the margins of the leaves, and the lamina cells were considered. For the genus, the arrangement of the stomata and the differentiation of the basal marginal leaf cells were considered. The species was defined based on morphological characteristics such as the presence and characteristics of the sporophyte, size, and shape of the capsule, hairiness of the calyptra, and the quantity, arrangement, shape, and coloration of the teeth of the exostome.

3.2. MAGNETIC MEASUREMENTS

Magnetic measurements were carried out at the Environmental Magnetism laboratory of IFAS (CIFICEN, UNCPBA, Argentina) and the Laboratory of Paleomagnetism at the IGc (UNAM, México). Measurements of mass-specific magnetic susceptibility (χ) and the frequency dependence (χ_{fd}%) were done using a susceptibility meter (MS2, Bartington Instruments Ltd.) connected to the MS2B dual frequency sensor (465 and 4650 Hz) and the MS2G. The anhysteretic remanent magnetization (ARM) was acquired by superimposing a DC field of 90 μT to an AF peak of 100 mT using a partial ARM (pARM) device attached to a shielded demagnetizer (Molspin Ltd.).

Anhysteretic susceptibility (χ_{ARM}) was determined using linear regression for ARM acquired

http://dx.doi.org/10.18268/BSGM2024v76n3a040324

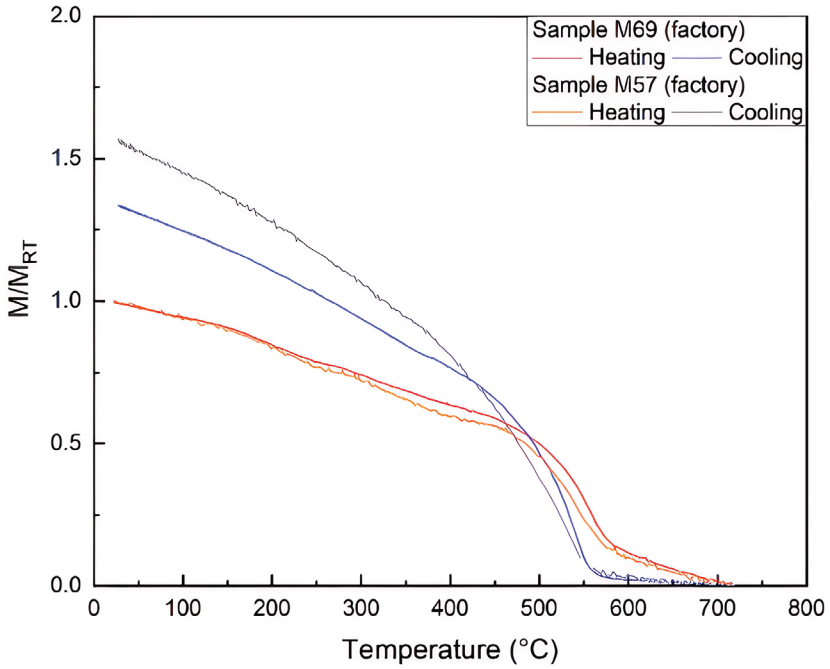

Figure 2 **Thermomagnetic curves for two representative moss samples from the studied area: sample M69 y M59 corresponds to a site near a metallurgical factory. The arrows indicate the Curie temperature estimated using the second derivative of M (T).**

at different DC bias fields (7.96, 47.75, and 71.8 A/m). The χ_{ARM}/χ was also determined. IRM (acquisition and backfield) studies were carried out with an ASC Scientific model IM-10-30 pulse magnetizer. After each step for ARM and IRM, the remanent magnetization was measured by a Molspin Ltd. Minispin fluxgate spinner magnetometer. The S-ratio (-IRM-300mT/SIRM), remanent coercivity (H_{cr}), and SIRM/χ were also determined. A small amount of moss (< 50 mg) was used to measure magnetic hysteresis loops and remanence measurements in fields between -2 and 2 T at room temperature (RT) using a Princeton Measurement Corporation Micromag 2900 AGM system equipped with a 2 T magnet. Saturation remanence (M_{rs}), saturation magnetization (M_s), coercive force (H_c), H_{cr}, and the ratios M_{rs}/M_s and H_{cr}/H_c were calculated.

Thermomagnetic measurements were carried out on some samples using a homemade horizontal magnetic translation balance (Escalante and Böhnel, 2011). Measurements were performed in the air using a magnetic field of 500 mT. Each sample was heated to about 720°C and then cooled to room temperature (RT) with a controlled heating/cooling rate of 30°C min^{-1}.

3.3. LIBS AND SCANNING ELECTRON MICROSCOPY ANALYSIS

The moss samples were incinerated in muffle to 475°C for 24 hours to eliminate all organic material and their preservation. For each sample, 1.5 g of material was homogenized with calcium oxide (4.5 g) and 3 ml of distilled water. The mixture was compressed to 140 MPa for 1 minute to form pellets of 3.5 cm^3 (diameter: 3 cm – thickness: 0.5 cm). LIBS measurements were carried out in the LIBS laboratory of IFAS (CIFICEN, Argentina). Spectroscopy studies were made using an Nd:YAG laser (Continuum Surelite II, λ = 1064 nm, 7 ns pulse FWHM, 100 mJ/pulse, repetition rate of 2 Hz) was focused at a right angle to the surface of the samples with a lens (100 mm focal length) in order to generate the plasmas in air atmospheric pressure.

http://dx.doi.org/10.18268/BSGM2024v76n3a040324

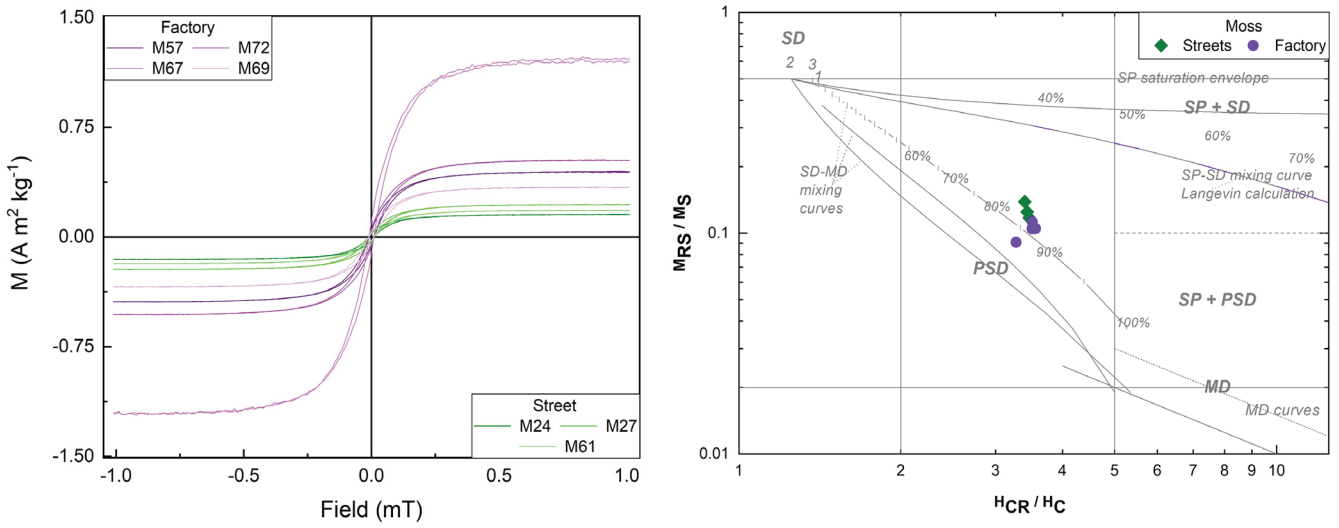

Figure 3 a) Magnetic hysteresis loops for seven moss samples collected from the street area (M24, M27, and M61) and near the factory area (M57, M72, M67, and M69). b) Day plot for moss samples from the studied area, and dashed lines indicate magnetite mixing lines (after Dunlop, 2002).

The pellets were rotated to avoid the formation of a deep crater by the ablation process, thus improving the reproducibility of measurements. The line profiles of plasma emission were collected in a perpendicular direction to the laser beam by a lens (200 mm focal length) and focused into the entrance slit of a monochromator (Jobin Yvon THR 1500, Czerny-Turner configuration, resolution of R = 300,000 in a double passage at λ = 300 nm, 1.5 m focal length, 2000 lines/mm holographic grating, entrance and exit slits = 100 µm). The light was detected by a photomultiplier (PM, Hamamatsu 1P28) whose signal was time-resolved and averaged with a Box-Car (Princeton Research Systems Inc. modules SR 280, SR 250, SR 200, and SR 245).

Finally, the spectra were recorded and processed by a PC. This experimental setup provided a good spectral resolution that allowed suitable recording of individual line profiles, free of spectral interference of other elements, at low concentrations. The final records studied have a range of 0.1 nm. Strong lines of elements of environmental interest, such as Si, Al, Cu, Mn, Fe, and Ti, were searched in the study samples (National Institute of Standards and Technology, 2019). The intensities of such emission lines were relatively appreciable and complied with the thin plasma model (Corney, 1977; Lochte-Holtgreven, 1968).

From these studies, only elements were selected in their neutral states, and the line profiles were measured with a delay time of 4 µs except for the case of Al, where it was 5 µs, with a gate time of 0.6 µs. A Lorentzian function adjusted the resulting emission lines for each element to obtain the area under the curve and, thus, the net emission intensities.

Moss samples were examined by scanning electron microscopy (SEM) using a Phillips microscope, model XL30. This microscope also allowed us to analyze the elemental composition of each specimen by X-ray energy dispersive spectroscopy (EDS) with an EDAX model DX4 (detection limit 0.5%).

http://dx.doi.org/10.18268/BSGM2024v76n3a040324

Table 1. Descriptive statistics for moss. N - number of samples.

Variable	N	Mean	s.d.	Median	Minimum	Maximum
χ (10^{-8} m^3kg^{-1})	84	187.1	92.8	168.5	72.9	667.8
ARM (10^{-6} Am^2kg^{-1})	84	581.2	165.4	562.8	283.4	1016.3
χ_{ARM} (10^{-8} m^3kg^{-1})	84	815.6	227.9	790.6	394.4	1416.7
SIRM (10^{-3} Am^2kg^{-1})	84	24.3	13.0	22.1	10.3	91.5
S-ratio	84	--	--	--	0.88	1
H_{cr} (mT)	84	34.6	2.2	34.7	28.5	38.8
SIRM/χ (kA/m)	84	13.0	1.6	12.9	8.6	23.9
χ_{fd}% (%)	84	2.9	1.2	2.9	0.3	6.6
χ_{ARM}/χ	84	4.7	1.2	4.7	2.1	7.5

4. Results and discussion

4.1. MOSS SPECIES

The moss species studied was identified as *Orthotrichum diaphanum* Brid., commonly growing on the bark of urban trees. It presents a greenish-brown color with greyish zones, rarely reaching a height of more than 1 cm. Stem leaves appear erect when dry. They have capsules surpassing the set of stems, pale and smooth, and recurved teeth in the peristome (Fuertes *et al.*, 1996). *O. diaphanum* is a species of wide distribution throughout the Holarctic region and South America. In addition, it is a eukaryotic species, which is to say that the range of conditions of the physical environment where it can live is wide. According to this and its preference for sites rich in nitrogen, *O. diaphanum* is abundant in urban environments, where elements in suspension are common (Casas *et al.*, 2006).

4.2. MAGNETIC PARTICLE PROPERTIES

The M (T) measurements are shown in Figure 2 for two representative samples collected near two metallurgical industries (M69 and M57). The thermomagnetic curves between RT and 720 °C have different slopes along heating and cooling runs. Curie temperatures (T_C) were estimated using the RockMagAnalyzer software (Leonhardt, 2006), using the second derivative of M (T). In sample M69, it is possible to observe two phases, one between RT and 600 ° C, with T_C = 575 °C, and another between 600 and 720 °C with T_C = 710 °C. Sample M57 has Curie temperatures of 571 °C and 710 °C. The T_Cs ≈ 570 °C suggested the dominance of magnetite. Changes in magnetization from 600 °C suggest the presence of other magnetic minerals, such as hematite, maghemite (Dankers, 1978), or iron (Gubbins and Herrero-Bervera, 2007). In both samples, the cooling runs were above the heating runs, suggesting the neoformation of ferrimagnetic minerals after the heating process (Magiera *et al.*, 2013; Paoli *et al.*, 2017).

The magnetic hysteresis curves for seven moss samples collected from factory areas (location are indicated in Figure S1, Supplementary Material) are shown in Figure 3a. The saturation is reached at around 250 mT, and the S-ratio ranges between 0.88 and 1 (Table 1), indicating the dominance of ferrimagnetic minerals (Thompson and Oldfield, 1986; Evans and Heller, 2003). Among ferrimagnetic minerals, magnetite is determined by H_c values of 9.6 – 10.5 mT and the H_{cr} values (mean = 34.6 mT; standard deviation, s.d. = 2.2 mT, Table

http://dx.doi.org/10.18268/BSGM2024v76n3a040324

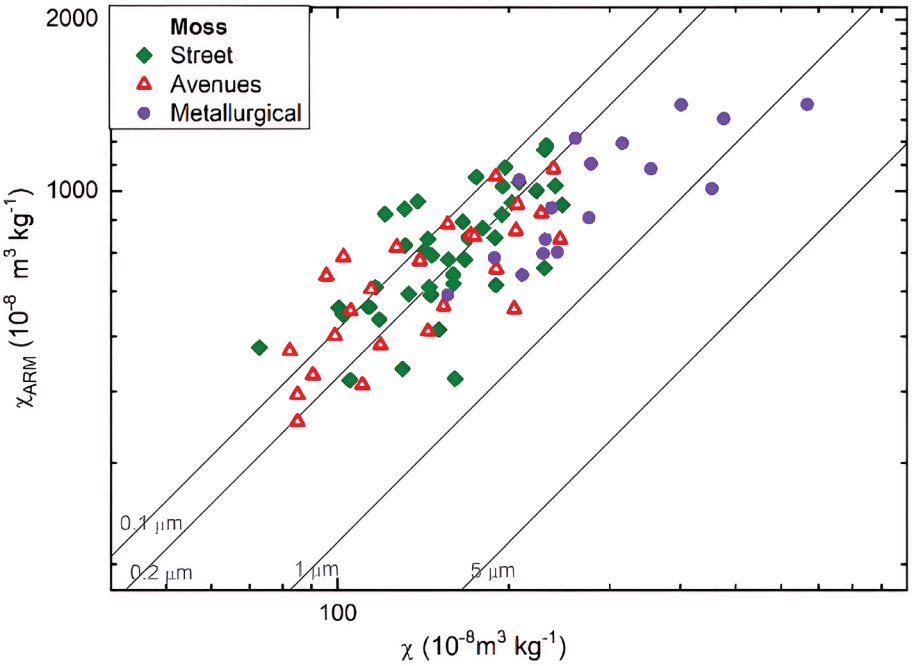

Figure 4 χ_{ARM} **versus** χ **for moss samples collected from the urban area of Tandil.**

1) (Peters and Dekkers, 2003).

The samples are in the pseudo-single domain (PSD) region of Day's plot (Figure 3b). Considering the mixing lines for single domain (SD) + multidomain (MD), mixtures of magnetite (Dunlop, 2002), samples with an MD contribution of 80 – 90% is observed. Samples corresponding to the industry have higher MD contributions (85%) than those from streets (80 – 85%). The comparison of the ratios of H_{cr}/H_c and M_{rs}/M_r, obtained in the moss samples studied, is found in the area corresponding to the (titano) magnetites. These values are similar to those reported by Marié *et al.* (2016) using lichens as biomonitors. Salo and Mäkinen (2014) obtained similar results for transplanted moss samples in Harjavalta (Finland).

Magnetic grain sizes were estimated using the calibration lines of the King's Plot (King *et al.*, 1982). Samples collected close to the metallurgical industries have magnetic grain sizes of about 0.2–5 μm (Figure 4), which agree with particles from the industrial emissions reported by Marié *et al.* (2016). Samples corresponding to sites from avenues and streets have finer particle sizes (about 0.1–1 μm), consistent with the AMP from vehicular emissions (Chaparro *et al.*, 2020).

Descriptive statistics for magnetic parameters and ratios are shown in Table 1. Values of the magnetic concentration dependent parameters ranged between 72.9 and 667.8 $\times 10^{-8}$ m^3kg^{-1} for χ, and between 10.3 and 91.5 $\times 10^{-3}$ Am^2kg^{-1} for SIRM. A similar variation is observed for the other concentration-dependent magnetic parameters ARM and χ_{ARM}, which are significantly correlated (Table S1 and Figure S2, Supplementary Material). The magnetic grain size-dependent parameters, *i.e.*, χ_{ARM}/χ and χ_{fd}%, varied from 2.1–7.5 and 0.3–7.5%, respectively. The lowest values of these parameters are associated with coarser magnetic particles and with high values of concentration-dependent magnetic parameters. The latter is observed through negative significant correlations between χ, SIRM, χ_{ARM}/χ, and χ_{fd}% (Table S1, Supplementary Material).

http://dx.doi.org/10.18268/BSGM2024v76n3a040324

Table 2. Name, sample site, magnetic parameters, and elements by magnetic techniques and LIBS are shown, respectively, for moss samples collected in the urban area of Tandil City. ND (not detected). Correlation analysis between magnetic and element contents are detailed, and significant correlations at the 0.01 (**) and 0.05 (*) level are shown.

Sample	Site	Magnetic parameters						LIBS Intensity (a.u.)					
		χ (10^{-8} m^3kg^{-1})	ARM (10^{-6} A m^2kg^{-1})	χ_{ARM} (10^{-8} m^3kg^{-1})	SIRM (10^{-3}A m^2kg^{-1})	χ_{ARM}/χ	H_{cr} (mT)	Fe	Mn	Al	Cu	Ti	Si
M35	Street	230.7	533.4	732.4	29.3	3.2	30.5	0.56	ND	2.11	2.38	10.33	7.20
M52	Street	223.5	721.6	1001.1	28.9	4.5	34.8	0.67	1.70	4.95	3.94	19.30	7.42
M74	Street	197.0	783.2	1099.1	27.3	5.6	35.7	0.77	4.15	2.40	3.29	6.01	4.90
M37	Street	169.6	596.5	828.2	21.2	4.8	34.4	1.02	2.09	4.96	15.71	15.65	7.651
M71	Factory	454.5	727.5	1008.3	64.9	2.2	31.8	5.67	2.72	4.88	14.91	13.00	9.27
M72	Factory	188.4	539.5	764.1	26.5	4.0	36.0	0.66	0.42	4.74	4.04	15.30	5.67
M76	Street	241.2	736.6	1022.4	31.3	4.2	33.2	0.93	5.69	4.86	6.36	7.53	7.58
M65	Street	131.3	570.1	802.5	18.3	6.1	36.0	0.85	ND	1.48	0.05	16.00	5.03

Pearson's coefficients							
		χ	ARM	χ_{ARM}	SIRM	χ_{ARM}/χ	H_{cr}
	Fe	0.916**	--	--	0.938**	--	--
	Mn	--	--	--	--	--	--
	Al	--	--	--	--	--	--
	Cu	--	--	--	--	--	--
	Ti	--	--	--	--	--	--
	Si	0.767*	--	--	0.712*	-0.793*	-0.723*

4.3. ELEMENT COMPOSITION AND MORPHOLOGY OF PARTICLES

Emission lines with wavelengths corresponding to Si, Al, Cu, Mn, Fe, and Ti were analyzed from LIBS results. An example of the Cu I (324.75 nm) and Fe I (404.58 nm) emission lines of sample M71 is shown in Figure S3 (Supplementary Material). Table S2 (Supplementary Material) details the selected emission lines for the different elements (sample M71). Figure 5 and Table 2 show the intensities of elements' emission lines of detected elements and magnetic parameters. It should be noted that in the case of the elements that were not detected (ND), no signal records were found concerning the background, which does not guarantee their non-existence, but these elements are below the detection limit for this technique.

The semi-quantitative analysis shows the presence of minerals such as Si and Al that are part of the earth's crust, to which Fe and Mn could be added. In terms of emission intensity, Fe shows its highest proportion in the M71 sample (5.67 a.u.), corresponding to a sample collected near a metallurgical factory, where this element is part of the production process. Concerning Cu values, a marked increase can also be observed in samples obtained close to metallurgical factories, such as M37 (15.71 a.u.) and M71 (14.91 a.u.), and areas with high vehicular traffic. Ali *et al.* (2012), Pandey *et al.* (2012) and Sharma *et al.* (2008) found an increase of heavy metals in vegetables associated with vehicular traffic and also due to the atmospheric deposition of particles in suspension. Dala-Paula *et al.* (2018) evaluated the concentration of PTEs in lettuce grown in urban areas and found an increase in Cu, Pb, and Cd. On the other hand, Ti was measured with high intensity, which could be associated with the emission caused by industries of iron alloys or other metals, according to Bayala and D'Angelo (2022).

Among the studied elements, Fe and Si domi-

http://dx.doi.org/10.18268/BSGM2024v76n3a040324

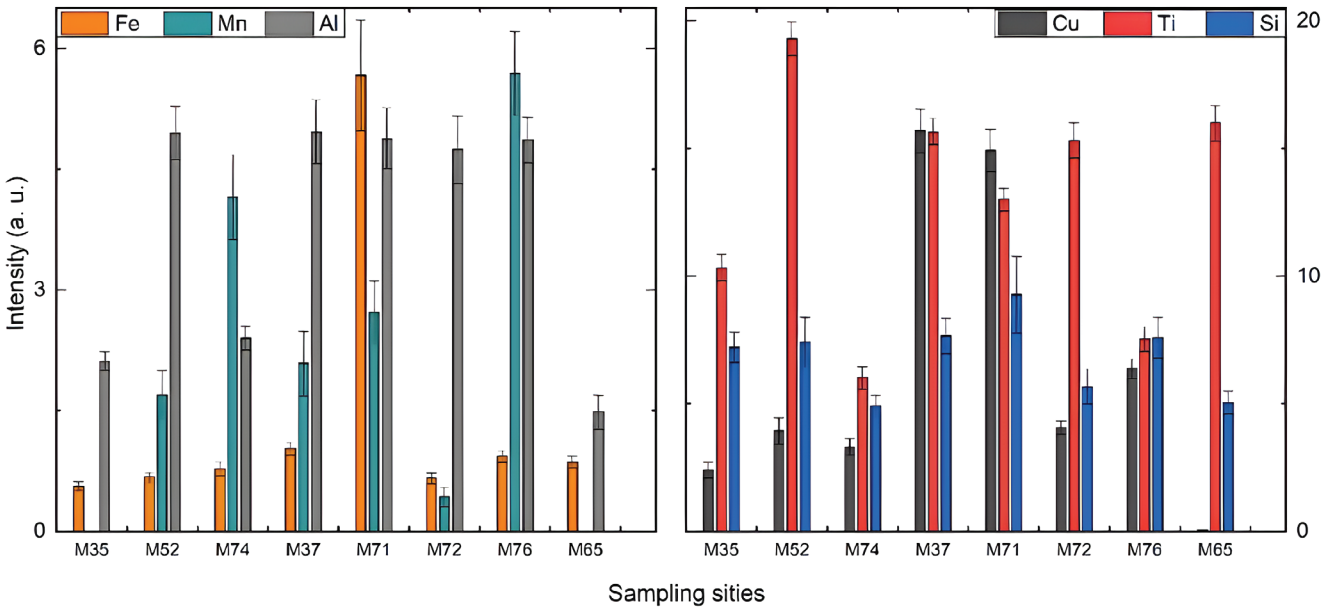

Figure 5 **Intensities of the Fe, Mn, Al, Cu, Ti, and Si emission lines for selected samples.**

nate spherules produced by metallurgical factories and traffic emissions (Chaparro *et al.*, 2013). In this study, they significantly correlate with the concentration-dependent magnetic parameters χ ($R = 0.92$, $p < 0.01$, and 0.77, $p < 0.05$) and SIRM ($R = 0.94$, $p < 0.01$, and 0.71, $p < 0.05$, Table 2). Also, Si correlates negatively with χ_{ARM}/χ ($R = -0.79$, $p < 0.05$) and H_{cr} ($R = -0.72$, $p < 0.05$, Table 2).

Spherules and various particles of different shapes and sizes are observed by SEM for samples from two factories (Figures 6a, 6b, 6d, 6e, and 6f) and from an avenue (Figure 6c). In most samples, spherules of varying diameters (2–10 µm) and anthropogenic particles (magnetic and non-magnetic) of various sizes are observed: large particles (15–20 µm), spherules of 1–10 µm and fine particles (< 5 µm).

The main component of the spherules determined by EDS is Fe (57.7 – 95.2 wt%), and in lower proportions, O, Al, Si, Ca, Mn, and Zn were found. Due to their structure and morphology, they are iron oxides of anthropogenic origin, consistent with Kim *et al.* (2007) for samples from industrialized sites with vehicular influence. Angular particles with sizes between 5 - 50 µm (Figure 6c) with small particles adhered to their surface showed Ti, K, Al, Si, O, and Fe, the iron with the highest proportion. Kim *et al.* (2007) and Chaparro *et al.* (2010) have reported similar results in samples obtained in areas with the influence of vehicle-derived pollutants. Bobrova and Vasil'ev (2023) have studied moss samples near metallurgical industries and reported the presence of spherical and detrital particles with high Fe, Ti, Mg, Ni, and Cr content, suggesting that mosses passively accumulate particulate PTEs and can be used to estimate the spatial distribution and sources of pollutants.

4.4. MAGNETIC PARTICLE DISTRIBUTION AND COMPARISON BETWEEN MOSS AND LICHEN SPECIES

The highest values of the magnetic concentration dependent parameters ($\chi = 667.8 \times 10^{-8}$ m^3kg^{-1}, and SIRM $= 91.5 \times 10^{-3}$ Am^2kg^{-1}) correspond to

http://dx.doi.org/10.18268/BSGM2024v76n3a040324

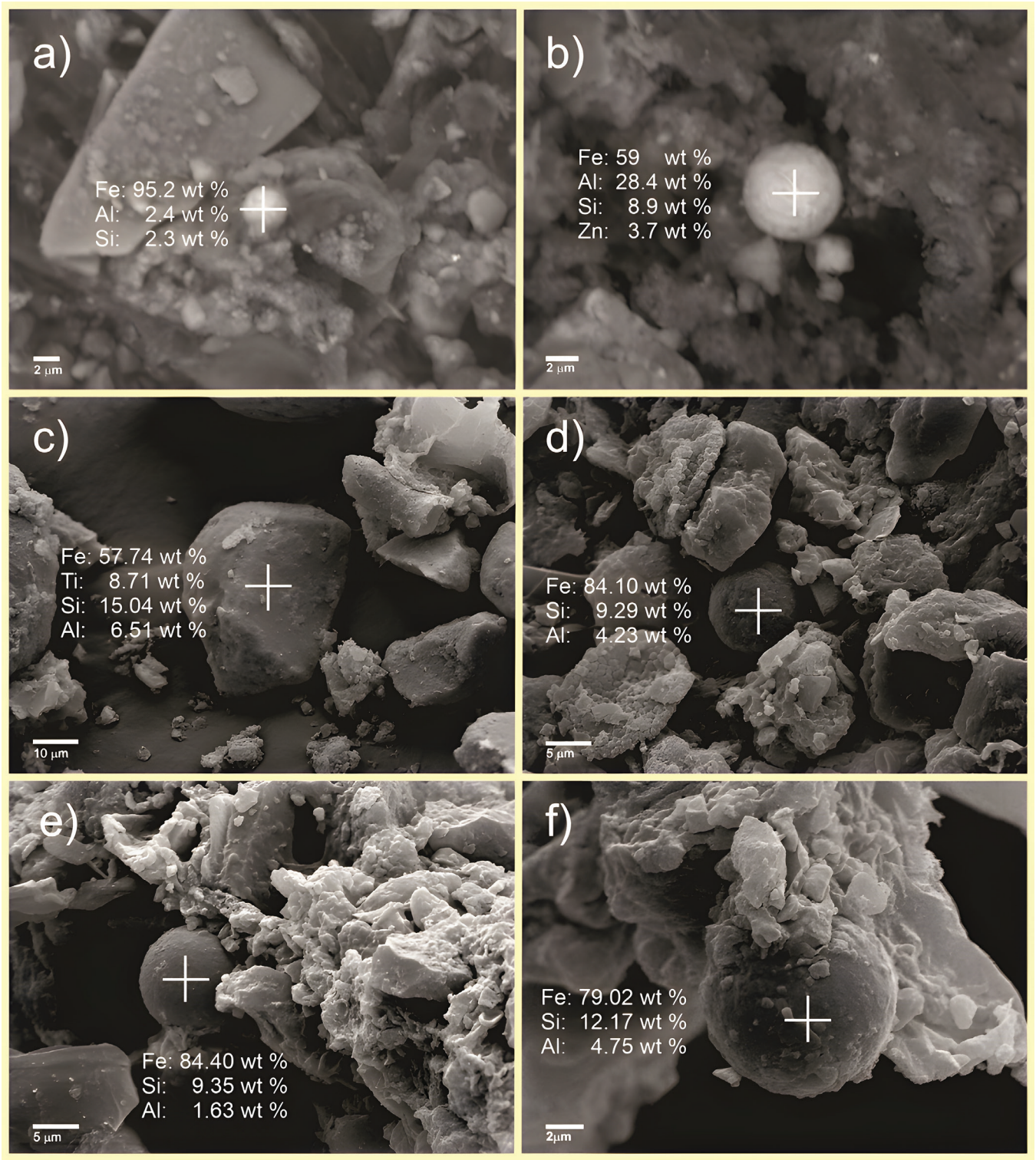

Figure 6 SEM-EDS analysis of samples from sites near two factories (a-b) and (d-f) and a sample collected on an avenue (c).

http://dx.doi.org/10.18268/BSGM2024v76n3a040324

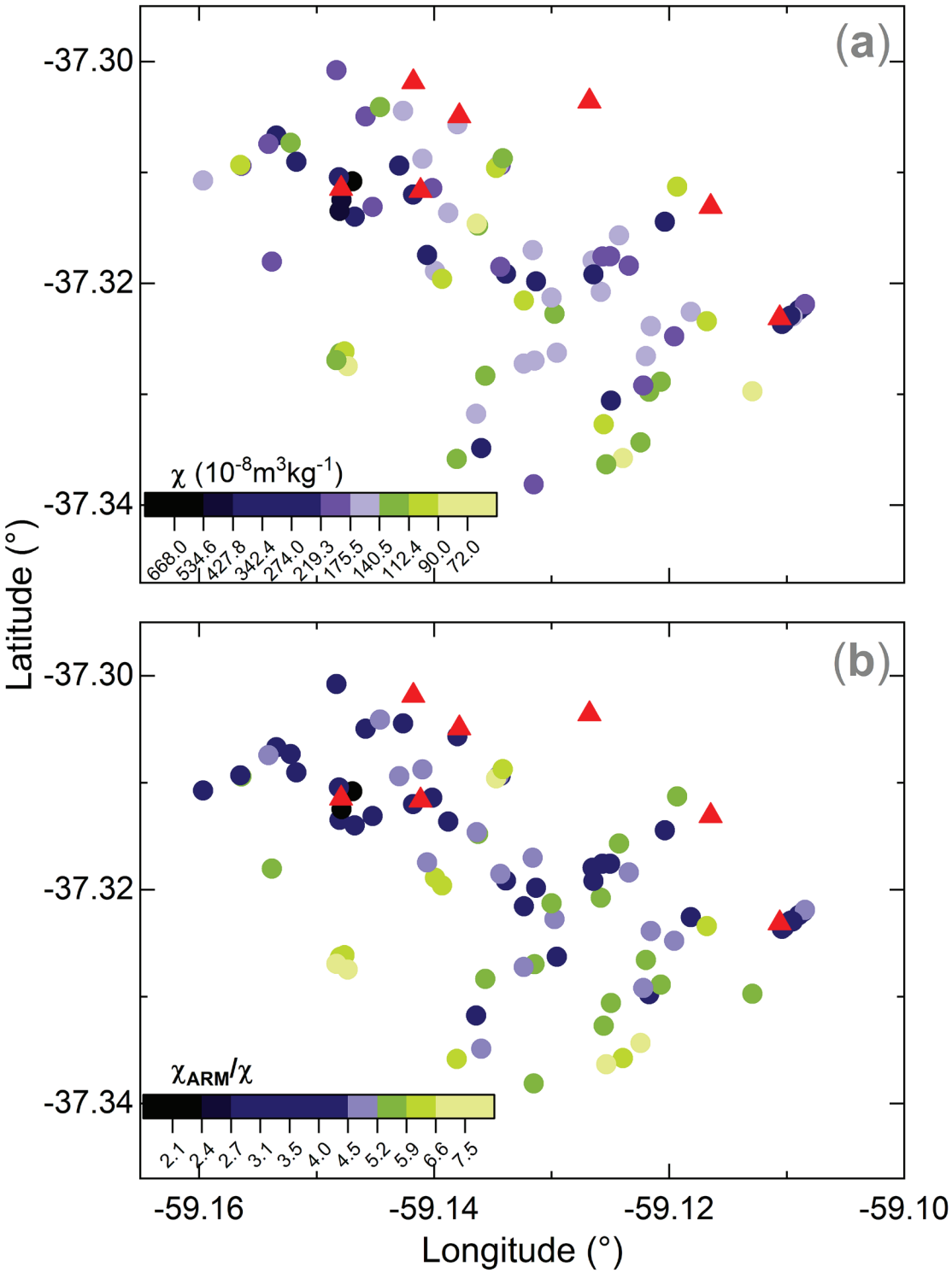

Figure 7 Distribution of the mass-specific magnetic susceptibility χ (a) and the anhysteretic ratio χ_{ARM}/χ (b). High χ values, corresponding to a high contribution of magnetic particles, delineate areas with high vehicular traffic and industrial (red triangles) influence. Low χ_{ARM}/χ values (coarser magnetic particles) are found in areas close to industries and avenues with high vehicular traffic.

http://dx.doi.org/10.18268/BSGM2024v76n3a040324

Table 3. Kruskal-Wallis test for moss samples (M, this study) and lichen samples (Marié *et al.*, 2016). Statistical differences in median values are indicated. YES indicates that differences are significant at the 0.05 level.

	Median of M samples (N = 84)	Median of L samples (N = 180)	Chi-Square	DF	Prob>Chi-Square	Differences at the 0.05 level
χ (10^{-8} m^3kg^{-1})	168.5	86.8	79.34	1	5.23E-19	YES
χ_{ARM} (10^{-8} m^3kg^{-1})	790.6	415.4	104.85	1	1.31E-24	YES
SIRM (10^{-3} Am^2kg^{-1})	22.1	11.8	78.23	1	9.15E-19	YES
H_{cr} (mT)	34.7	34.5	0.81	1	3.69E-01	NO
SIRM/χ (kA/m)	12.9	12.6	4.41	1	3.57E-02	YES
χ_{ARM}/χ	4.7	4.4	4.43	1	3.53E-02	YES

sites near one metallurgical industry (Figure 7a). The median values of these areas (Met), *i.e.*, χ = 261.5 $\times10^{-8}$ m^3kg^{-1}, and SIRM = 34.8 $\times10^{-3}$ Am^2kg^{-1}, are up to two-fold higher than avenues (Ave) and street (St) areas. According to the Kruskal-Wallis test, such differences between Met and Ave and St areas are statistically significant Table S3 (Supplementary Material).

The areas influenced by vehicle emissions have high χ_{ARM}/χ and χ_{fd}% (relatively fine magnetic particles), *i.e.*, median values of χ_{ARM}/χ = 4.8 and χ_{fd}% = 2.7% for Ave and χ_{ARM}/χ = 5.0 and χ_{fd}% = 3.3% for St (Table S3, Supplementary Material), and high values of concentration-dependent magnetic parameters. Sites near industries also have high values of concentration-dependent magnetic parameters but lower median values of χ_{ARM}/χ = 3.5 and χ_{fd}% = 2.2%, indicating coarser magnetic particles (Figure 7b). Chaparro *et al.* (2013) have observed a similar behavior, a decrease in the magnetic particle sizes with the distance to the industrial emission source. Although there are significant differences between metallurgical sites and avenues and street sites, this is not true between avenues and street sites (Table S3, Supplementary Material).

Magnetic measurements indicate that both epiphytes, mosses (M), and lichens (Marié *et al.*, 2016) can be used to study air particle pollution. The statistically significant differences in the median values using the Kruskal-Wallis test for magnetic parameters and ratios between these two epiphytes are shown in Table 3, revealing that mosses accumulate AMP effectively. Salo *et al.* (2012) studied the efficiency of another lichen (*Hypogymnia physodes*) and moss (*Sphagnum papillosum*) species as collectors of anthropogenic magnetic particles and the relationship of χ with PTEs contamination. They proved that both bioindicators' species could be used to study particle pollutants' spatial distribution in urban (Turku City) and industrial (Harjavalta City) areas of SW Finland. The medians of the concentration-dependent magnetic parameters (χ, χ_{ARM} and SIRM) of both species present a significant difference between them, observing that the values of mosses (median of χ = 168.5 $\times10^{-8}$ m^3kg^{-1} and SIRM = 22.1 $\times10^{-3}$ Am^2kg^{-1}) are double those of lichens (Table 3). When comparing the medians of the magnetic mineralogy-dependent parameter, *i.e.*, H_{cr} = 34.5 mT for lichens and H_{cr} = 34.7 mT for mosses, an insignificant difference is observed between mosses and lichens. These results indicate that *O. diaphanum* collects higher AMP contents than lichens,

http://dx.doi.org/10.18268/BSGM2024v76n3a040324

which may be related to morphological characteristics of *P. pilosum*, such as topography, micro-scale roughness of the thallus surface, deformation, and its retention capacity (Marié *et al.*, 2018). In addition, each species collects a similar population of AMP emitted by traffic and industry.

This study indicates that the *Orthotrichum diaphanum* Brid. can be used to assess airborne particle pollution. However, using this moss species for other magnetic biomonitoring needs a previous evaluation of its distribution in the target area.

5. Conclusions

The analysis of magnetic parameters in moss samples of *Orthotrichum diaphanum* Brid. indicates the presence of magnetite as the primary trapped airborne magnetic particles. The magnetic grain size estimation shows that avenues and street sites have finer magnetic particles (0.1–1 μm) than sites close to metallurgical industries with coarser particles of 0.2–5 μm. Compositional and morphological studies show that these Fe-rich particles are spherules and irregular particles of different sizes. These airborne magnetic particles correspond to the inhalable PM category, which is risky for human health.

LIBS studies confirm the presence of elements, such as Fe, Mn, Al, Cu, Ti, and Si, associated with traffic and industrial emissions as primary sources of particle pollutants. Fe and Si significantly correlate with the concentration-dependent magnetic parameters χ and SIRM.

An integral analysis of the magnetic parameters χ, SIRM, χARM/χ, and χ_{fd}% allows for identifying areas close to metallurgical factories and with high traffic most affected by airborne magnetic particle contamination.

The statistical comparison of magnetic parameters between moss species *O. diaphanum* and the lichen species *P. pilosum* shows the efficiency of both mosses and lichens for magnetic biomonitoring of air particle pollution.

Acknowledgements

The authors thank UNCPBA, UNAM, and CONICET for their financial support. This contribution was supported by the Bilateral CONICET/ CONACYT Project Res. 1001/14 - 5131/15 (Marcos Chaparro) and the CONICET Project PUE-2017-22920170100004CO. Part of the reported data was obtained during MAEC stays supported by project project DGAPA PAPIIT IG-101921. The authors also thank Dr. Alicia Irurzun and Mr. Pablo Zubeldía (CICPBA) for their help in the field, Ing. Jorge Escalante and Dr. Marina Vega González (Instituto de Geociencias, UNAM) for their help performing thermomagnetic and SEM-EDS studies.

Contributions of authors

(1) Conceptualization: DCM, LM; (2) Investigation: DCM, LM, MAEC, CD, JML, HB; (3)Writing of the original manuscript: DCM; (4) Writing of the corrected and edited manuscript: LM, MAEC, CD, JML, HB. All authors have read and agreed to the published version of the manuscript.

Conflict of interest

There is no conflict of interest.

Handling editor

Ana María Soler Arechalde

References

Ali, M.H.H., Al-Qahtani, K.M., 2012, Assessment of some heavy metals in vegetables, cereals and fruits in Saudi Arabian markets: Egyptian Journal of Aquatic Research, 38(1), 31-37. https://doi.org/10.1016/j.ejar.2012.08.002

Bayala, M.P., D'Angelo, C., 2022, Aplicación de la técnica LIBS en la detección de Ti en efluentes líquidos industriales: Anales AFA, 33(3), 65-69, https://doi.org/10.31527/

analesafa.2022.33.3.65

Bobrova, A.V., Vasil'ev A.A., 2023, Magnetic particles in soils and epiphytes in the zone of influence of a ferrous metallurgy factory in the city of Perm: Geography, Environment, Sustainability, 16(1), 157-162. https://doi.org/10.24057/2071-9388-2022-058

Calasans, C.F., Malm, O., 1997, Elemental mercury contamination survey in a chlor-alkali plant by the use of transplanted Spanish moss, Tillandsia usneoides (L.): Science of the Total Environment, 208(3), 165-177. https://doi.org/10.1016/S0048-9697(97)00281-7

Casas, C., Brugués, M., Cros, R.M., Sérgio, C., 2006, Handbook of mosses of the Iberian Peninsula and the Balearic Islands: illustrated keys to genera and species: Barcelona, Institut d'Estudis Catalans, 379 p.

Chaparro, M.A.E., 2021, Airborne particle accumulation and loss in pollution-tolerant lichens and its magnetic quantification: Environmental Pollution, 288, 117807. https://doi.org/10.1016/J.ENVPOL.2021.117807

Chaparro, M.A.E., Gogorza, C.G.S., Lavat, A., Pazos, S, Sinito, A.M., 2002, Preliminary results of magnetic characterisation of different soils in the Tandil Region (Argentina) affected by the pollution of metallurgical factory: European Journal of Environmental and Engineering Geophysics, 7, 35-58.

Chaparro, M.A.E., Marié, D.C., Gogorza, C.S.G., Navas, A., Sinito, A.M., 2010, Magnetic studies and scanning electron microscopy - X-ray energy dispersive spectroscopy analyses of road sediments, soils and vehicle-derived emissions: Studia Geophysica et Geodaetica, 54, 633-650. https://doi.org/10.1007/s11200-010-0038-2

Chaparro, M.A.E., Lavornia, J.M., Chaparro, M.A.E., Sinito, A.M., 2013, Biomonitors of urban air pollution: Magnetic studies and SEM observations of corticolous foliose and microfoliose lichens and their suitability for magnetic monitoring: Environmental Pollution, 172, 61-69. https://doi.org/10.1016/j.envpol.2012.08.006

Chaparro, M.A.E., Chaparro, M.A.E., Castañeda-Miranda, A.G., Marié, D.C., Gargiulo, J.D., Lavornia, J.M., Natal, M., Böhnel, H.N., 2020, Fine air pollution particles trapped by street tree barks: In situ magnetic biomonitoring: Environmental Pollution, 226, 115229. https://doi.org/10.1016/j.envpol.2020.115229

Corney, A., 1977, Atomic and Laser Spectroscopy: Oxford, Clarendon Press, 782 p.

Dala-Paula, B.M., Custódio, F.B., Knupp, E.A.N., Palmieri, H.E.L., Silva, J.B.B., Glória, M.B.A., 2018, Cadmium, copper and lead levels in different cultivars of lettuce and soil from urban agriculture: Environmental Pollution, 242(A), 383-389. https://doi.org/10.1016/j.envpol.2018.04.101

Dankers, P.H.M., 1978, Magnetic properties of dispersed natural iron-oxides of known grain-size: Nederland, State University of Utrecht, tesis doctoral, 142 p.

Dunlop, D.J., 2002, Theory and application of the day plot (M_{rs}/M_s versus H_{cr}/H_c) 1. Theoretical curves and tests using titanomagnetite data: Journal of Geophysical Research, 107(B3), EPM4-1-EPM4-22. http://dx.doi.org/10.1029/2001JB000486

Escalante, J.E., Böhnel, H.N., 2011, Diseño y construcción de una balanza de Curie: Geos, 31(1), 63.

Evans, M.E., Heller, F., 2003, Environmental magnetism: Principles and applications of enviromagnetics: USA, Elsevier Science, 299 p.

Fabian, K., Reimann, C., McEnroe, S.A., Willemoes-Wissing, B., 2011, Magnetic properties of terrestrial moss (Hylocomium splendens) along a north-south profile crossing the city of Oslo, Norway: Science of the Total Environment, 409(11), 2252-2260. https://doi.org/10.1016/j.scitotenv.2011.02.018

Fuertes, E., Burgaz, A.R., Escudero, A., 1996, Pre-climax epiphytic communities of bryophytes

http://dx.doi.org/10.18268/BSGM2024v76n3a040324

and lichens in Mediterranean forests from the Central Plateau (Spain): Vegetatio, 123, 139-151. https://doi.org/10.1007/bf00118267

Gradstein, S.R., Churchill, S. P., Salazar-Allen, N., 2001, Guide to the bryophytes of tropical America: Memoirs of the New York Botanical Garden, 86, 577 p.

Gubbins, D., Herrero-Bervera, E., (eds.), 2007, Encyclopedia of Geomagnetism and Paleomagnetism: Dordrecht, The Netherlands, Springer-Verlag, 1054 p.

Instituto Nacional de Estadística y Censos, 2023, Censo nacional de población, hogares y viviendas 2022: resultados provisionales (en línea): Ciudad Autónoma de Buenos Aires, Instituto Nacional de Estadística y Censos - INDEC, disponible en <https://www.censo.gob.ar/index.php/datos_provisionales/> , consultado 4 de septiembre de 2023.

Jordanova, D., Petrov, P., Hoffmann, V., Gocht, T., Panaiotu, C., Tsacheva, T., Jordanova, N., 2010, Magnetic signature of different vegetation species in polluted environment: Studia Geophysica et Geodaetica, 54, 417-442. https://doi.org/10.1007/s11200-010-0025-7

Kim, W., Doha, S.J., Park, Y.H., Yun, S.T., 2007, Two-year magnetic monitoring in conjunction with geochemical and electron microscopic data of roadside dust in Seoul, Korea: Atmospheric Environment, 41(35), 7627-7641. https://doi.org/10.1016/j.atmosenv.2007.05.050

King, J., Banerjee, S.K., Marvin, J., Özdemir, Ö., 1982, A comparison of different magnetic methods for determining the relative grain size of magnetite in natural materials: some results from lake sediments: Earth and Planetary Science Letters, 59(2), 404-419. https://doi.org/10.1016/0012-821x(82)90142-x

Leonhardt, R., 2006, Analyzing rock magnetic measurements: the Rock- MagAnalyzer1.0 software: Computers and Geosciences, 32(9), 1420-1431. https://doi.org/10.1016/j.cageo.2006.01.006

Lochte-Holtgreven, W., 1968, Measuring Plasmas: Plasma Diagnostics: Amsterdam, Interscience, 930 p.

Magiera, T., Gołuchowska, B., Jabłońska, M., 2013, Technogenic magnetic particles in alkaline dusts from power and cement plants: Water, Air and Soil Pollution, 224, 1389. https://doi.org/10.1007/s11270-012-1389-9

Mahapatra, B., Dhal, N.K., Dash, A.K., Panda, B.P., Panigrahi, K.C.S., Pradhan, A., 2019, Perspective of mitigating atmospheric heavy metal pollution: using mosses as biomonitoring and indicator organism: Environmental Science and Pollution Research, 26, 29620–29638. https://doi.org/10.1007/s11356-019-06270-z

Marié, D.C., Chaparro, M.A.E., Irurzun, M.A., Lavornia, J.M., Marinelli, C., Cepeda, R., Böhnel, H.N., Castañeda-Miranda, A.G., Sinito, A.M., 2016, Magnetic mapping of air pollution in Tandil city (Argentina) using the lichen *Parmotrema pilosum* as biomonitor: Atmospheric Pollution Research, 7(3), 513-520. https://doi.org/10.1016/j.apr.2015.12.005

Marié, D.C., Chaparro, M.A.E., Lavornia, J.M., Sinito, A.M., Castañeda-Miranda, A.G., Gargiulo, J.D., Chaparro, M.A.E., Böhnel, H.N., 2018, Atmospheric pollution assessed by in situ measurement of magnetic susceptibility on lichens: Ecological Indicators, 95(1), 831-840. https://doi.org/10.1016/j.ecolind.2018.08.029

National Institute of Standards and Technology, 2019, NIST Atomic Spectra Database Lines Form (en línea): USA, NIST, disponible en <https://physics.nist.gov/PhysRefData/ASD/lines_form.html>

Martino, L.J., D'Angelo, C.A., Marinelli, C., Cepeda, R., 2021, Identification and detection of pesticide in chard samples by laser-induced breakdown spectroscopy using chemometric methods: Spectrochimica Acta Part B: Atomic Spectroscopy, 177, 106031. https://doi.org/10.1016/j.sab.2020.106031

Martino, L.J., D'Angelo, C.A., 2022, Quantification of dimethoate and chlorpyrifos residues in green leafy vegetables by laser-induced breakdown spectroscopy: Spectrochimica Acta Part B: Atomic Spectroscopy, 195, 106485. https://doi.org/10.1016/j.sab.2022.106485

Pandey, R., Shubhashish, K., Pandey, J., 2012, Dietary intake of pollutant aerosols via vegetables influenced by atmospheric deposition and wastewater irrigation: Ecotoxicology and Environmental Safety, 76(1), 200-208. https://doi.org/10.1016/j.ecoenv.2011.10.004

Paoli, L., Winkler, A., Guttová, A., Sagnotti, L., Grassi, A., Lackovičová, A, Senko, D., Loppi, S., 2017, Magnetic properties and element concentrations in lichens exposed to airborne pollutants released during cement production: Environmental Science and Pollution Research, 24, 12063–12080. https://doi.org/10.1007/s11356-016-6203-6

Peters, C., Dekkers, M.J., 2003, Selected room temperature magnetic parameters as a function of mineralogy, concentration and grain size: Physics and Chemistry of the Earth, Parts A/B/C, 28(16-19), 659-667. https://doi.org/10.1016/s1474-7065(03)00120-7

Picone, N., 2014, Clima urbano de la ciudad de Tandil: República Argentina, Universidad Nacional del Sur, tesis doctoral, 147 p.

Picone, N., Campo, A.M., 2012, Variaciones estacionales de la isla térmica en la ciudad de Tandil, en IX Jornadas Nacionales de Geografía Física Bahía Blanca: Republica Argentina, 99-106.

Salo H., Mäkinen J., 2014, Magnetic biomonitoring by moss bags for industry-derived air pollution in SW Finland: Atmospheric Environment, 97, 19-27. https://doi.org/10.1016/j.atmosenv.2014.08.003

Salo, H., Bućko, M.S., Vaahtovuo, E., Limo, J., Mäkinen, J., Pesonen, L.J., 2012, Biomonitoring of air pollution in SW Finland by magnetic and chemical measurements of moss bags and lichens: Journal of Geochemical Exploration, 115, 69-81. https://doi.org/10.1016/j.gexplo.2012.02.009

Sharma, R.K., Agrawal, M., Marshall, F.M., 2008, Heavy metal (Cu, Zn, Cd and Pb) contamination of vegetables in urban India: A case study in Varanasi: Environmental Pollution, 154(2), 254-263. https://doi.org/10.1016/j.envpol.2007.10.010

Singh, J.P., Thakur, S.N., 2007, Laser-Induced Breakdown Spectroscopy: Amsterdam, Elsevier, 454 p. https://doi.org/10.1016/B978-0-444-51734-0.X5001-7

Sosa, B.S., 2015, Contaminación ambiental por material particulado y compuestos orgánicos volátiles en la ciudad de Tandil, provincia de Buenos Aires: República Argentina, Facultad de Ciencias Exactas, Universidad Nacional de La Plata, tesis doctoral, 230 p. https://doi.org/10.35537/10915/45123

Thompson, R., Oldfield, F., 1986, Environmental Magnetism: London, Allen & Unwin, 227 p. https://doi.org/10.1007/978-94-011-8036-8

Zhou, X., Chen, Q., Liu, C., Fang, Y., 2017, Using moss to assess airborne heavy metal pollution in Taizhou, China: International Journal of Environmental Research and Public Health, 14(4), 430. https://doi.org/10.3390/ijerph14040430

http://dx.doi.org/10.18268/BSGM2024v76n3a040324

Supplementary Material

Table S1. Pearson's coefficients between magnetic parameters of moss samples (N = 84). Significant correlations are indicated at the 0.05 (*) and 0.01 (**) levels.

	χ	ARM	χ_{ARM}	SIRM	χ_{ARM}/χ	χ_{fd}%	SIRM/χ	H_{cr}	S-ratio
χ	1								
ARM	0.75**	1							
χ_{ARM}	0.76**	0.99**	1						
SIRM	0.98**	0.79**	0.79**	1					
χ_{ARM}/χ	-0.66**	--	--	-0.57**	1				
χ_{fd}%	-0.35**	--	--	-0.33**	0.39**	1			
SIRM/χ	--	0.29**	--	0.22*	0.39**	--	1		
H_{cr}	-0.33**	--	--	-0.25*	0.60**	--	0.28*	1	
S-ratio	0.27*	--	--	0.22*	-0.29**	--	--	-0.44**	1

Table S2. Measurement of elements and their respective emission lines for sample M71

Elements	Emission lines
Fe I	404.58
Mn I	403.28
Si I	288.16
Al I	309.27
Cu I	324.75
Ti I	521.03

http://dx.doi.org/10.18268/BSGM2024v76n3a040324

Table S3. Median values and Kruskal-Wallis test for moss samples from metallurgical areas (Met), avenues (Ave), and streets (St). Statistical differences in median values of magnetic parameters are indicated. YES indicates that differences are significant at the 0.05 level.

	Met (N = 17)	Ave (N = 26)	St (N = 41)	
χ ($10^{-8}m^3kg^{-1}$)	261.5	141.8	159.4	
SIRM (10^{-3} Am^2kg^{-1})	34.8	18.4	21.0	
χ_{ARM}/χ	3.5	4.8	5.0	
χ_{fd}% (%)	2.2	2.7	3.3	
SIRM/χ (kA/m)	13.2	12.9	12.9	
H_{cr} (mT)	33.2	35.3	35.1	
Kruskal-Wallis Test				
	Chi-Square	**DF**	**Prob>Chi-Square**	**Differences at the 0.05 level**
χ				
Met-Ave	22.3	1	2E-06	YES
Met-St	24.6	1	7E-07	YES
Ave-St	1.7	1	2E-01	no
SIRM				
Met-Ave	21.3	1	4E-06	YES
Met-St	22.6	1	2E-06	YES
Ave-St	1.0	1	3E-01	no
χ_{ARM}/χ				
Met-Ave	16.2	1	6E-05	YES
Met-St	20.7	1	5E-06	YES
Ave-St	0.0	1	9E-01	no
χ_{fd}%				
Met-Ave	6.0	1	1E-02	YES
Met-St	8.2	1	4E-03	YES
Ave-St	0.9	1	3E-01	no
SIRM/χ				
Met-Ave	1.4	1	2E-01	no
Met-St	1.2	1	3E-01	no
Ave-St	0.0	1	9E-01	no
H_{cr}				
Met-Ave	8.7	1	3E-03	YES
Met-St	7.9	1	5E-03	YES
Ave-St	0.1	1	8E-01	no

http://dx.doi.org/10.18268/BSGM2024v76n3a040324

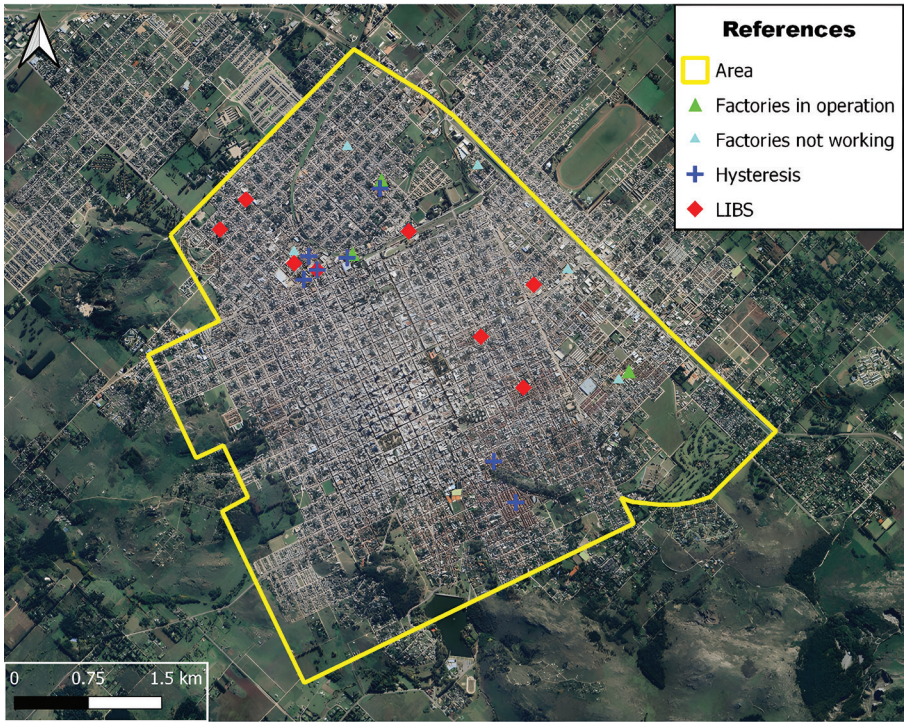

Figure S1 Study area, hysteresis samples (blue crosses), LIBS Samples (red diamond), Factories in operation (green triangles) and factories not working (small light blue triangles) are shown.

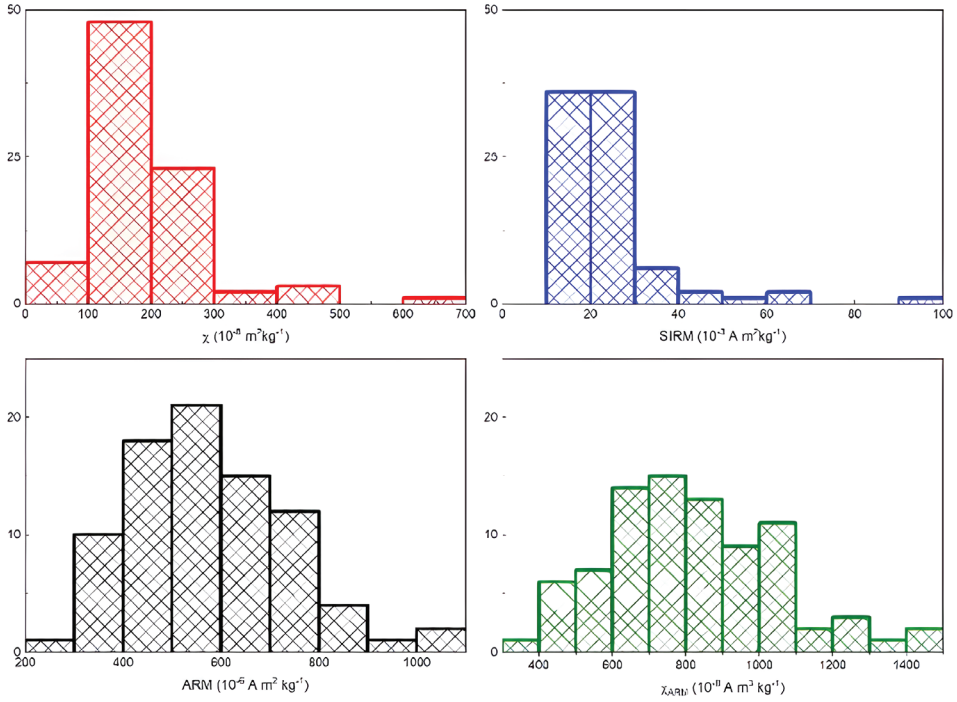

Figure S2 Distribution of concentration-dependent magnetic parameters: χ (red), SIRM (green), ARM (black), χ_{ARM} (olive).

http://dx.doi.org/10.18268/BSGM2024v76n3a040324

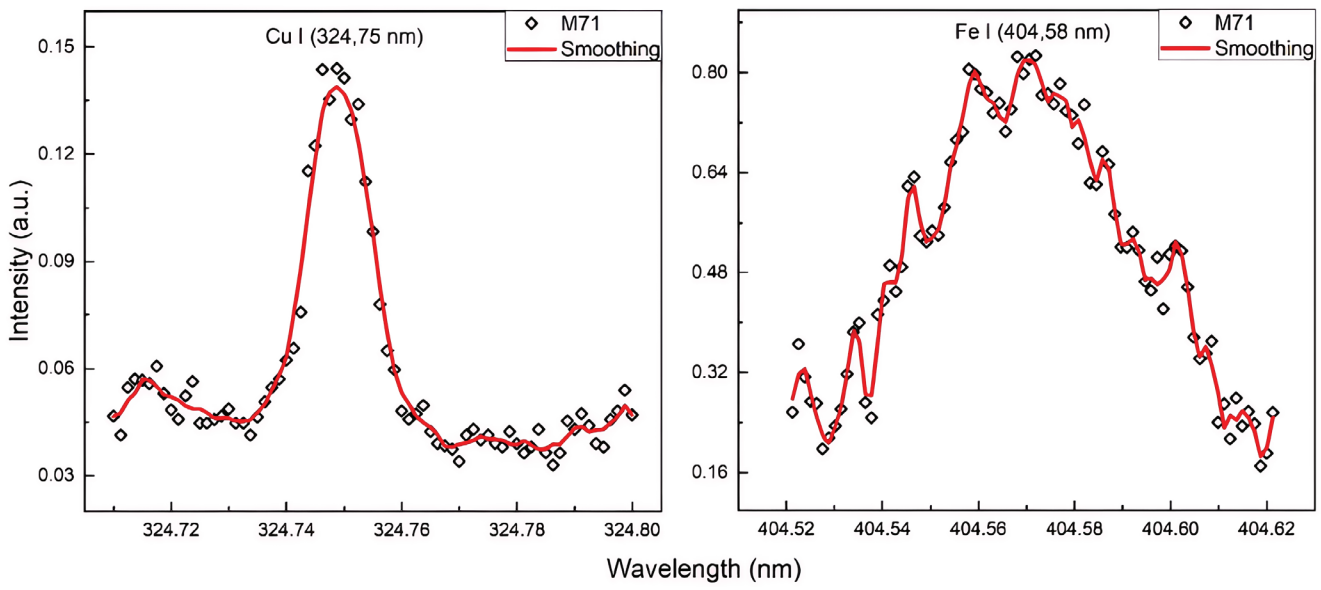

Figure S3 Cu I emission lines (324.75 nm) and Fe I emission lines (404.58 nm) for a sample from the factory area (M71).